Large-scale vortices in rapidly rotating Rayleigh-Bénard convection

Céline Guervilly, David Hughes and Chris Jones

Department of Applied Mathematics, University of Leeds, UK

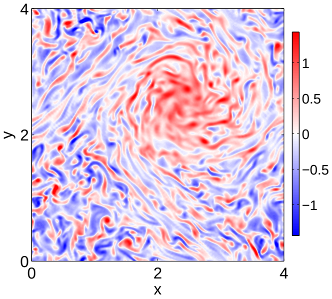

Large-scale vortices in convective layers

- Numerical models of **rotating compressible thermal convection** in a local f-plane model (Chan 2007, Chan & Mayr 2013, Käpylä et al. 2011, Mantere et al. 2011): long-lived, box-size vortices for large rotation rate and near the poles.

cyclone:
negative temperature anomaly

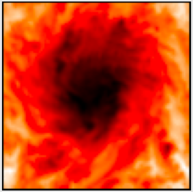

anticyclone:
positive temperature anomaly

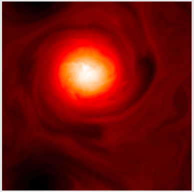

Large-scale vortices in convective layers

- Numerical models of **rotating compressible thermal convection** in a local f-plane model (Chan 2007, Chan & Mayr 2013, Käpylä et al. 2011, Mantere et al. 2011): long-lived, box-size vortices for large rotation rate and near the poles.

cyclone:
negative temperature anomaly

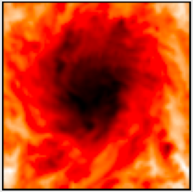

anticyclone:
positive temperature anomaly

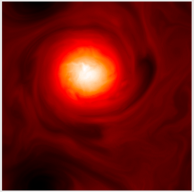

- **Reduced model of Boussinesq convection** in a local Cartesian domain in the limit of small Rossby number (Julien et al. 2012): depth-invariant box-size vorticity dipole, increases the efficiency of the heat transfer

depth-averaged axial vorticity

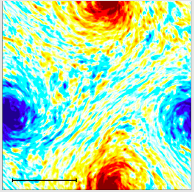

Outline

1. Structure of large-scale vortices in rotating Boussinesq convection
2. Domain of existence in parameter space
3. Cyclone/anticyclone asymmetry
4. Energy transfer to large scales
5. Effect on the heat transfer

Rotating Rayleigh-Bénard convection

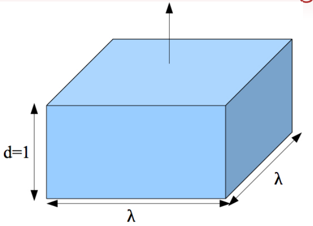

- 3D Cartesian layer of Boussinesq fluid
- periodic in the horizontal directions
- rotating about the vertical axis, rotation rate: Ω
- temperature difference between top (cold) and bottom (hot): ΔT
- aspect ratio between horizontal/vertical box sizes: λ

$$
\begin{aligned}
&\frac{\partial \mathbf{u}}{\partial t} + \mathbf{u}\cdot\nabla\mathbf{u} + \frac{Pr}{Ek}\mathbf{e}_z \times \mathbf{u} = -\nabla p + Pr\,Ra\,\theta\mathbf{e_z} + Pr\nabla^2\mathbf{u},\\
&\nabla\cdot\mathbf{u} = 0,\\
&\frac{\partial \theta}{\partial t} + \mathbf{u}\cdot\nabla\theta = u_z + \nabla^2\theta.
\end{aligned}
$$

Boundary conditions:

$$
\begin{aligned}
&\theta = 0,\\
&u_z = 0, \qquad \frac{\partial u_x}{\partial z} = \frac{\partial u_y}{\partial z} = 0.
\end{aligned}
$$

Input parameters:

$$
Ra = \frac{\alpha g \Delta T d^3}{\kappa\nu}, \quad Pr = \frac{\nu}{\kappa} = 1, \quad Ek = \frac{\nu}{2\Omega d^2}.
$$

Emergence of the large-scale vortices

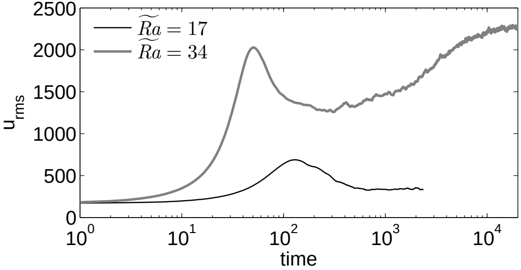

(in units of $1/2\Omega$)

$\widetilde{Ra} = RaEk^{4/3}$
$Ek = 5 \times 10^{-6}$
$\lambda = 1$

slow growth of the kinetic energy for $\widetilde{Ra} = 34$ and saturation after about 10% of the global viscous timescale

Emergence of the large-scale vortices

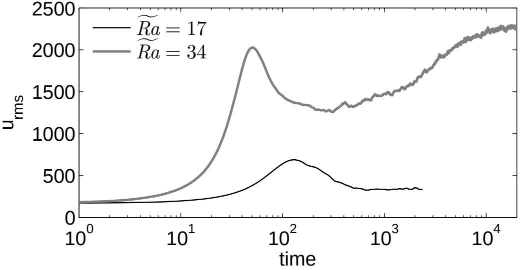

(in units of $1/2\Omega$)

$\widetilde{Ra} = RaEk^{4/3}$
$Ek = 5 \times 10^{-6}$
$\lambda = 1$

slow growth of the kinetic energy for $\widetilde{Ra} = 34$ and saturation after about 10% of the global viscous timescale

time = 14.4

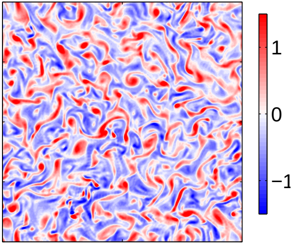

Movie: horizontal cross-section of the axial vorticity starting after the development of the convective instability
(parameters: $Ek = 10^{-4}$, $\widetilde{Ra} = 37$, $\lambda = 4$)

Slow growth of the kinetic energy $\Rightarrow$ formation of a large-scale vortex

Emergence of the large-scale vortices

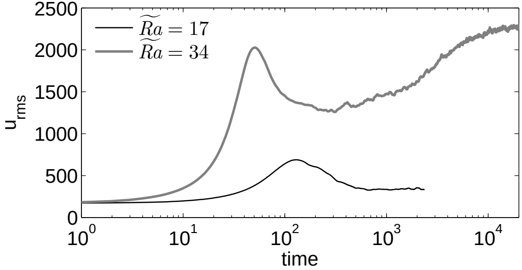

(in units of $1/2\Omega$)

$\widetilde{Ra} = RaEk^{4/3}$
$Ek = 5 \times 10^{-6}$
$\lambda = 1$

slow growth of the kinetic energy for $\widetilde{Ra} = 34$ and saturation after about 10% of the global viscous timescale

Horizontal and vertical cross-sections of the axial vorticity:

$\widetilde{Ra} = 17$ $\widetilde{Ra} = 34$

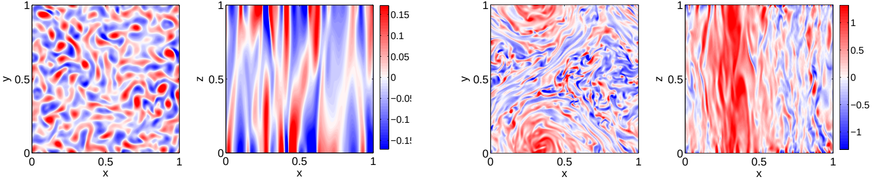

- vortex aligned with rotation axis and mostly z-invariant
- grows to the largest horizontal scale permitted
- periodic horizontal boundary conditions: horizontal average of ω_z is zero
- consists essentially of horizontal motions

Evolution of the velocity

$$Ro_z = \frac{\langle u_z^2 \rangle^{1/2}}{2\Omega d} \quad \text{and} \quad Ro = \frac{\langle u_x^2 + u_y^2 + u_z^2 \rangle^{1/2}}{2\Omega d}.$$

S1: $Ek = 10^{-4}$, $\lambda = 1$
S2: $Ek = 10^{-4}$, $\lambda = 2$
S3: $Ek = 10^{-4}$, $\lambda = 4$
S4: $Ek = 10^{-5}$, $\lambda = 1$
S5: $Ek = 5 \times 10^{-6}$, $\lambda = 1$
$\widetilde{Ra} = Ra Ek^{4/3}$

Evolution of the velocity

$$Ro_z = \frac{\langle u_z^2 \rangle^{1/2}}{2\Omega d} \quad \text{and} \quad Ro = \frac{\langle u_x^2 + u_y^2 + u_z^2 \rangle^{1/2}}{2\Omega d}.$$

S1: $Ek = 10^{-4}$, $\lambda = 1$
S2: $Ek = 10^{-4}$, $\lambda = 2$
S3: $Ek = 10^{-4}$, $\lambda = 4$
S4: $Ek = 10^{-5}$, $\lambda = 1$
S5: $Ek = 5 \times 10^{-6}$, $\lambda = 1$
$\widetilde{Ra} = RaEk^{4/3}$

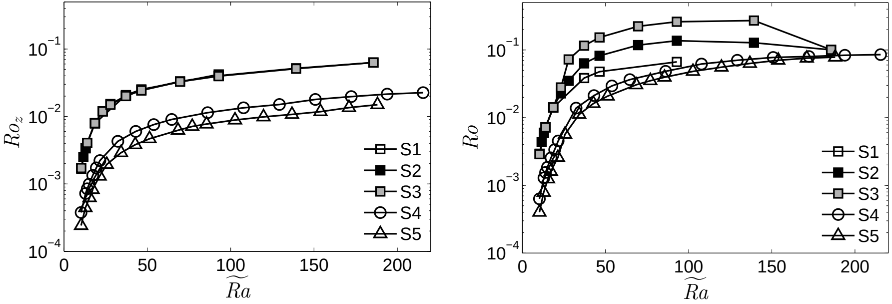

Ro_z increases monotonically with $\widetilde{Ra}$, always smaller than 0.1, does not depend on λ

Ro decreases in series S2–S3 for $\widetilde{Ra} \gtrsim 150$, depends on λ

The amplitude of the horizontal flows does not follow the evolution of the amplitude of the vertical flows.

Domain of existence

Comparison of the amplitudes of horizontal flows with vertical flows:

$$\Gamma = \frac{\langle u_x^2 + u_y^2 + u_z^2 \rangle}{3\langle u_z^2 \rangle} = \frac{Ro^2}{3Ro_z^2}$$

Domain of existence

Comparison of the amplitudes of horizontal flows with vertical flows:

$$\Gamma = \frac{\langle u_x^2 + u_y^2 + u_z^2 \rangle}{3\langle u_z^2 \rangle} = \frac{Ro^2}{3Ro_z^2}$$

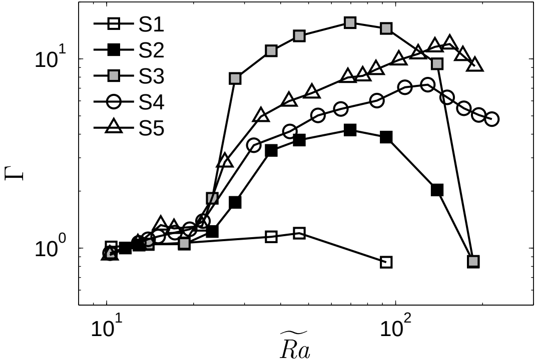

S1: $Ek = 10^{-4}$, $\lambda = 1$
S2: $Ek = 10^{-4}$, $\lambda = 2$
S3: $Ek = 10^{-4}$, $\lambda = 4$
S4: $Ek = 10^{-5}$, $\lambda = 1$
S5: $Ek = 5 \times 10^{-6}$, $\lambda = 1$
$\widetilde{Ra} = RaEk^{4/3}$

- $\Gamma > 1$ for $\widetilde{Ra} \gtrsim 20$ (onset of convection: $\widetilde{Ra} = 8.8$)
- Γ decays for large thermal forcings

Domain of existence: emergence

Measure of the level of turbulence of the convective flow:

$$Re_z = \frac{Ro_z}{Ek} = \frac{\langle u_z^2 \rangle^{1/2} d}{\nu}$$

Domain of existence: emergence

Measure of the level of turbulence of the convective flow:

$$Re_z = \frac{Ro_z}{Ek} = \frac{\langle u_z^2 \rangle^{1/2} d}{\nu}$$

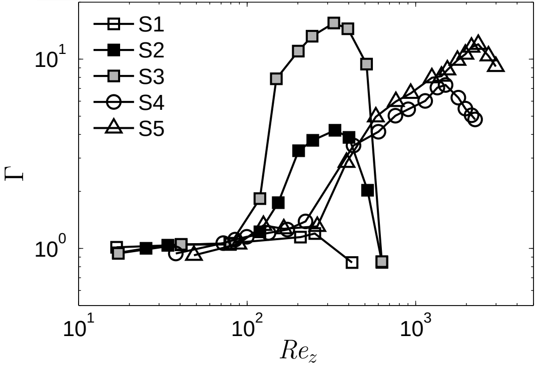

S1: $Ek = 10^{-4}$, $\lambda = 1$
S2: $Ek = 10^{-4}$, $\lambda = 2$
S3: $Ek = 10^{-4}$, $\lambda = 4$
S4: $Ek = 10^{-5}$, $\lambda = 1$
S5: $Ek = 5 \times 10^{-6}$, $\lambda = 1$
$\Gamma = Ro^2/(3Ro_z^2)$

- Sharp increase of Γ for $Re_z \approx 300$ for $\lambda = 1$ and for $Re_z \approx 100$ for $\lambda = 4$
- Decrease of Γ occurs at increasing values of Re_z for decreasing Ek $\rightarrow$ due to a transition from a rotationally-dominated convection regime to a weakly-rotating convection regime?

Domain of existence: decay

Measure of the influence of rotation on a flow:

$$Ro_z^l = \frac{\langle u_z^2 \rangle^{1/2}}{2\Omega l_h} = \frac{Ro_z}{l_h/d}$$

Domain of existence: decay

Measure of the influence of rotation on a flow:

$$Ro_z^l = \frac{\langle u_z^2 \rangle^{1/2}}{2\Omega l_h} = \frac{Ro_z}{l_h/d}$$

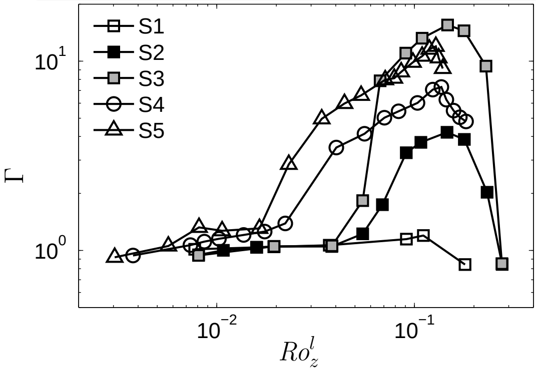

S1: $Ek = 10^{-4}$, $\lambda = 1$
S2: $Ek = 10^{-4}$, $\lambda = 2$
S3: $Ek = 10^{-4}$, $\lambda = 4$
S4: $Ek = 10^{-5}$, $\lambda = 1$
S5: $Ek = 5 \times 10^{-6}$, $\lambda = 1$
$\Gamma = Ro^2/(3Ro_z^2)$

- Ro_z^l monotonically increases with $\widetilde{Ra}$
- decrease of Γ occurs for a similar value of Ro_z^l, about 0.15

Horizontal cross-sections of the axial vorticity at $z = 0.25$ ($Ek = 10^{-4}$, $\widetilde{Ra} = 37$):

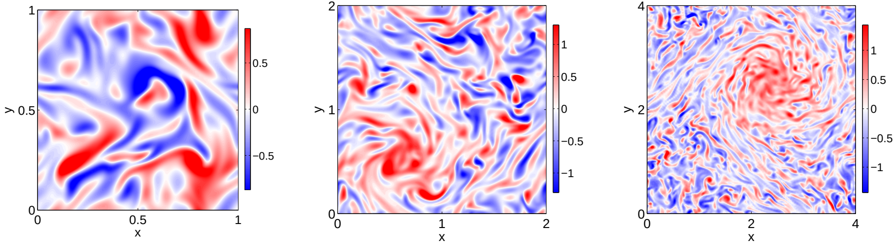

$\lambda = 1$ $\lambda = 2$ $\lambda = 4$

Domain of existence: effect of the aspect ratio

Kinetic energy spectrum in the horizontal directions with $k_h = (k_x^2 + k_y^2)^{1/2}$ ($Ek = 10^{-4}$, $\widetilde{Ra} = 37$):

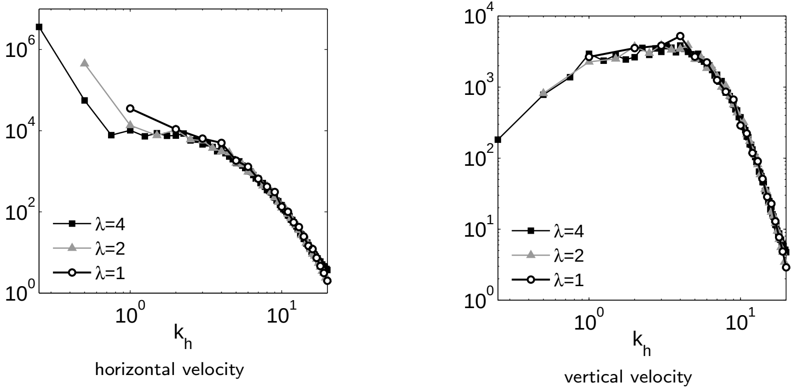

- Kinetic energy spectra show that the horizontal flow is dominated by the smallest permitted horizontal wavenumber, for all λ.
- As λ increases, the amplitude of the smallest horizontal wavenumber becomes larger.

Domain of existence: Summary

1. Significant level of convectively-driven turbulence is required: $Re_z \gtrsim 100 - 300$ depending on the aspect ratio; this value of Re_z is reached for Ra three times above the onset of convection.

2. Convection remains in a regime strongly dominated by the rotation: $Ro_z^l \lesssim 0.15$.

3. An energy transfer to the largest scale takes place even for moderate scale separation between the horizontal extent of the convective cells (l_h) and the horizontal box size (λ) (smallest scale separation considered: $\lambda / l_h \approx 4$)

Preference for cyclonic vorticity (1)

Horizontal cross-section of ω_z

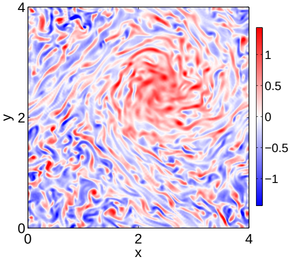

Preference for cyclonic vorticity (1)

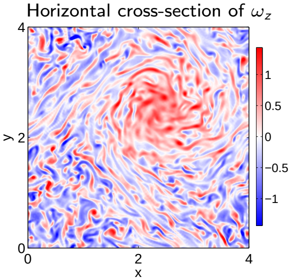

- Compressible convection (Chan & Mayr 2013; Käpylä et al. 2011): Large-scale anticyclones for $Ro_z < 0.06$ and large-scale cyclone for $Ro_z < 0.25$

Preference for cyclonic vorticity (1)

Horizontal cross-section of ω_z

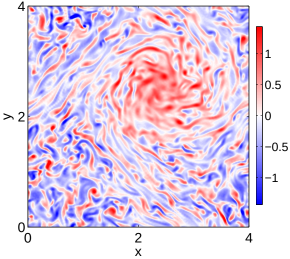

- Compressible convection (Chan & Mayr 2013; Käpylä et al. 2011): Large-scale anticyclones for $Ro_z < 0.06$ and large-scale cyclone for $Ro_z < 0.25$
- Periodic horizontal boundary conditions so horizontal mean of ω_z is zero
- Axial vorticity skewness:

$$S = \frac{\langle \omega_z^3 \rangle}{\langle \omega_z^2 \rangle^{3/2}}$$

Preference for cyclonic vorticity (1)

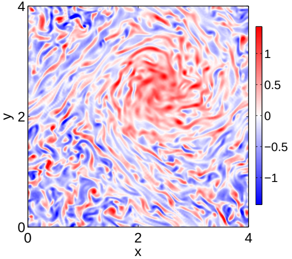

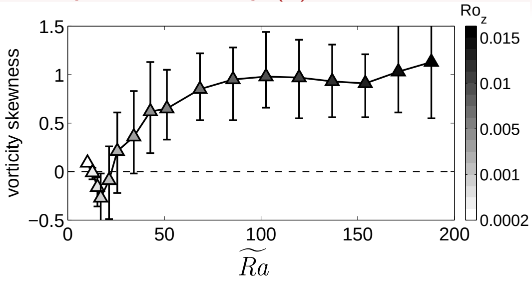

$Ek = 5 \times 10^{-6}$, $\lambda = 1$

- Compressible convection (Chan & Mayr 2013; Käpylä et al. 2011): Large-scale anticyclones for $Ro_z < 0.06$ and large-scale cyclone for $Ro_z < 0.25$
- Periodic horizontal boundary conditions so horizontal mean of ω_z is zero
- Axial vorticity skewness:

$$S = \frac{\langle \omega_z^3 \rangle}{\langle \omega_z^2 \rangle^{3/2}}$$

- For $\widetilde{Ra} > 21$, $S > 0$: cyclonic vorticity of large amplitude is more likely than anticyclonic vorticity
- Large-scale anticyclone due to compressibility effects?

Preference for cyclonic vorticity (2)

- Asymmetry between cyclones and anticyclones is common in turbulent 3D rotating systems (e.g. Hopfinger et al. 1982)
- Possibilities: (i) System cannot maintain large-scale anticyclone or (ii) both large-scale cyclones and anticyclones form but anticyclones are unstable

Preference for cyclonic vorticity (2)

- Asymmetry between cyclones and anticyclones is common in turbulent 3D rotating systems (e.g. Hopfinger et al. 1982)
- Possibilities: (i) System cannot maintain large-scale anticyclone or (ii) both large-scale cyclones and anticyclones form but anticyclones are unstable
- Stability of a large-scale anticyclone structure: **Movie**: at $t = 0$ inversion of the sign of vorticity

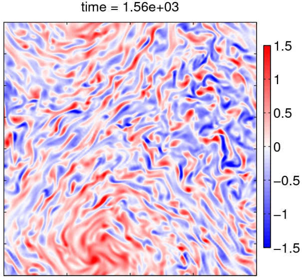

Preference for cyclonic vorticity (2)

- Asymmetry between cyclones and anticyclones is common in turbulent 3D rotating systems (e.g. Hopfinger et al. 1982)
- Possibilities: (i) System cannot maintain large-scale anticyclone or (ii) both large-scale cyclones and anticyclones form but anticyclones are unstable
- Stability of a large-scale anticyclone structure: **Movie**: at $t = 0$ inversion of the sign of vorticity

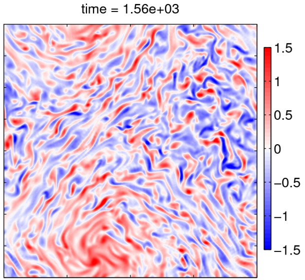

- Locally in the cyclone, $\omega_z \sim 2\Omega \Rightarrow$ absolute vorticity $\to 0$ in anticyclone $\Rightarrow$ large-scale anticyclone unstable to 3D perturbations (e.g. Lesieur et al. 1991)
- Anticyclone region: reduction of the rotation $\Rightarrow$ convection cells in the core are not anisotropic enough

Preference for cyclonic vorticity (3)

Reduced Boussinesq model (Julien et al. 2012): both cyclones and anticyclones of similar vorticity

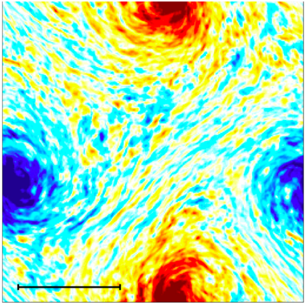

$$\frac{\partial \omega_z}{\partial t} + (\mathbf{u} \cdot \nabla)\omega_z = (2\Omega + \omega_z)\frac{\partial u_z}{\partial z} + (\boldsymbol{\omega}_H \cdot \nabla)u_z + \nu \nabla^2 \omega_z,$$

with $\boldsymbol{\omega}_H = (\omega_x, \omega_y, 0)$.

Small Rossby number limit: $\omega_z \ll 2\Omega \Rightarrow$ the system has no preference for cyclonic or anticyclonic flow.

Energy transfer to large scales (1)

$$\frac{\partial \omega_z}{\partial t} + (\mathbf{u}\cdot\nabla)\omega_z = (2\Omega + \omega_z)\frac{\partial u_z}{\partial z} + (\boldsymbol{\omega}_H \cdot \nabla)u_z + \nu\nabla^2\omega_z, \quad \text{with} \quad \boldsymbol{\omega}_H = (\omega_x, \omega_y, 0)$$

- No direct thermal forcing for the horizontal flows
- 2D inverse cascade or direct transfer from small scales?

Energy transfer to large scales (1)

$$\frac{\partial \omega_z}{\partial t} + (\mathbf{u} \cdot \nabla)\omega_z = (2\Omega + \omega_z)\frac{\partial u_z}{\partial z} + (\boldsymbol{\omega}_H \cdot \nabla)u_z + \nu\nabla^2\omega_z, \quad \text{with} \quad \boldsymbol{\omega}_H = (\omega_x, \omega_y, 0)$$

- No direct thermal forcing for the horizontal flows
- 2D inverse cascade or direct transfer from small scales?

Kinetic energy of the horizontal velocity
($Ek = 5 \times 10^{-6}$, $\lambda = 1$):

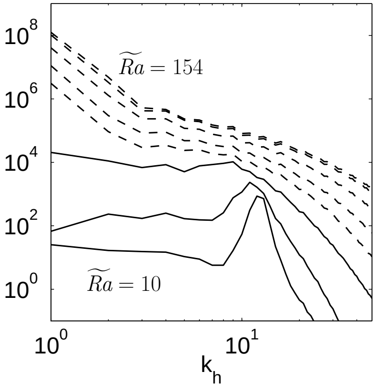

Energy transfer to large scales (1)

$$\frac{\partial \omega_z}{\partial t} + (\mathbf{u}\cdot\nabla)\omega_z = (2\Omega + \omega_z)\frac{\partial u_z}{\partial z} + (\boldsymbol{\omega}_H\cdot\nabla)u_z + \nu\nabla^2\omega_z, \quad \text{with} \quad \boldsymbol{\omega}_H = (\omega_x, \omega_y, 0)$$

- No direct thermal forcing for the horizontal flows
- 2D inverse cascade or direct transfer from small scales?

Kinetic energy of the horizontal velocity ($Ek = 5\times10^{-6}$, $\lambda = 1$):

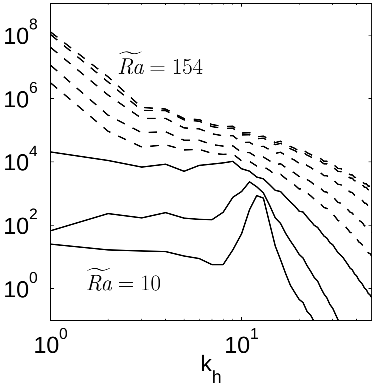

Kinetic energy in $1 \le k_h \le 12$ ($\widetilde{Ra} = 34$)

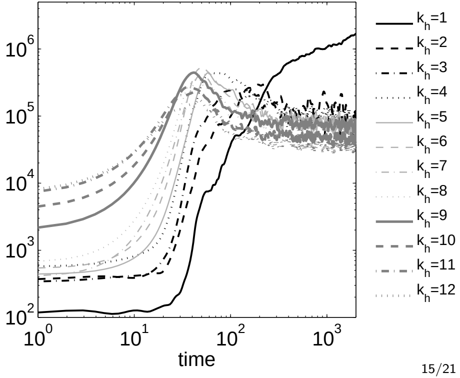

Energy transfer to large scales (2)

Filtered simulations
($Ek = 5 \times 10^{-6}$, $\widetilde{Ra} = 34$) : Suppress a range of wavenumbers (k_h, k_z) at each timestep

Case:	Full	A	B	C	D
$k_z = 0$	all	1	1	1	1
$k_z \neq 0$	all	all	≥ 6	≥ 15	≥ 21
ratio $k_h = 1/\text{total}$	0.81	0.77	0.91	0.73	0.03

($k_h = 12$: marginally stable mode at onset)

Kinetic energy in $k_h = 1$

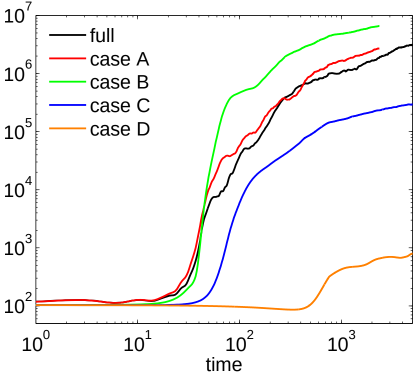

Suggests that the large-scale $k_z = 0$ mode:

- does not require the interaction of $k_z = 0$ modes (case A): not produced by 2D inverse cascade
- does not require the presence of intermediate wavenumbers (cases B-C)
- is produced by interactions of small-scale (typical convective size), z-dependent motions

Effect on the heat transfer (1)

- Compressible convection (Chan 2007, Kapyla et al. 2011): Large-scale cyclone associated with negative temperature anomaly
- Boussinesq system: symmetric temperature anomaly with respect to the mid-plane

Effect on the heat transfer (1)

- Compressible convection (Chan 2007, Kapyla et al. 2011): Large-scale cyclone associated with negative temperature anomaly
- Boussinesq system: symmetric temperature anomaly with respect to the mid-plane

Heat Flux: $q = -\left.\frac{\partial \theta}{\partial z}\right|_{z=1} + 1$

z-average axial vorticity:

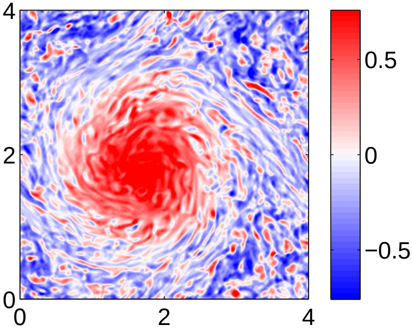

heat flux at the surface:

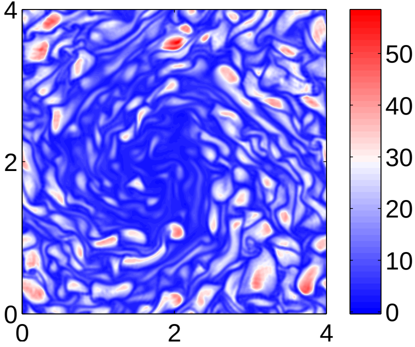

Parameters: $Ek = 10^{-4}$, $\widetilde{Ra} = 46$ and $\lambda = 4$

Time-average:

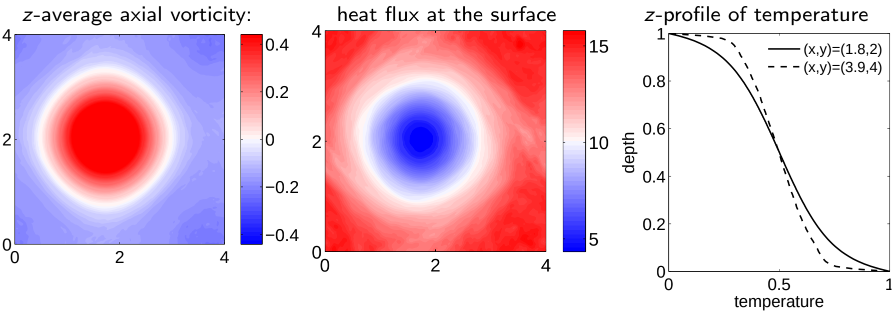

- Steeper vertical profile of temperature outside the cyclone in the bulk
- Vertical mixing of temperature is less efficient in the cyclone: increase of the rotation locally inhibits convection

Effect on the heat transfer (3)

Nusselt number = total heat flux across the layer/flux in absence of motion

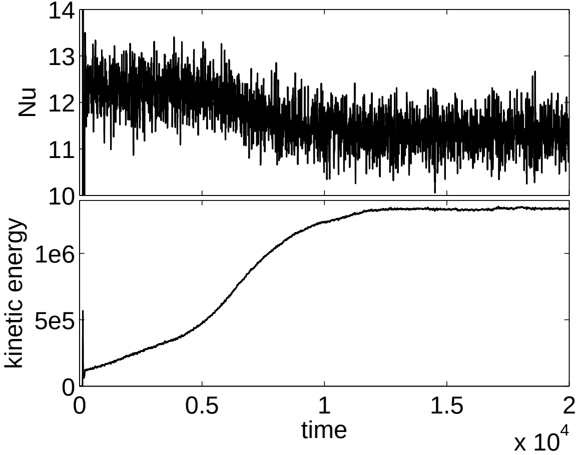

Parameters: $Ek = 10^{-4}$, $\widetilde{Ra} = 37$ and $\lambda = 4$

Reduced model of Julien et al. (2012): increase of the Nusselt number as the vorticity dipole forms.

Effect on the heat transfer (4)

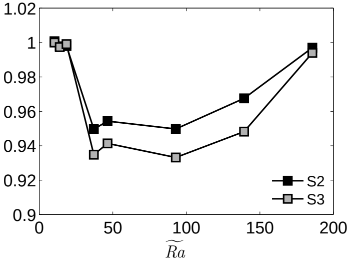

R_{Nu}, the ratio of the Nusselt number in series S2 and S3 to the Nusselt number in the series S1 for the same $\widetilde{Ra}$

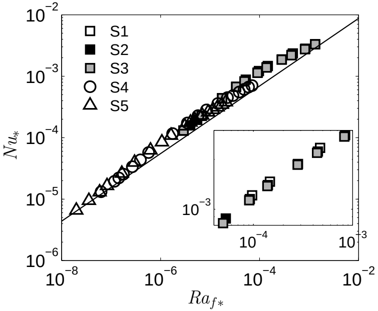

The solid line corresponds to $Nu_* = 0.11 Ra_{f*}^{0.55}$, which is the best fit to the data of Schmitz & Tilgner (2009)

Conclusions

1. Flow dominated by the emergence of a large-scale vortex at the box-size (nearly depth-invariant, always cyclonic) for $Re_z \gtrsim 100 - 300$ and $Ro_z^l \lesssim 0.15$.

2. Filtered simulations: Large-scale vortex produced by interactions of small-scale (typical convective size), z-dependent, convective motions. These motions need to be sufficiently anisotropic or the vortex does not form.

3. Large-scale cyclone decreases the efficiency of the vertical heat transfer.